

Monitoring of Cure-Induced Strain of an Epoxy Resin by Fiber Bragg Grating Sensor

Margit Harsch,¹ József Karger-Kocsis,² Florian Herzog¹

¹Robert Bosch GmbH, Immenstadt, Germany

²Institut für Verbundwerkstoffe GmbH, Kaiserslautern, Germany

Received 15 March 2007; accepted 8 May 2007

DOI 10.1002/app.27096

Published online 25 September 2007 in Wiley InterScience (www.interscience.wiley.com).

ABSTRACT: In this study, we present a method to detect cure-induced strain in an epoxy resin (EP) with a Fiber Bragg Grating (FBG) sensor. By embedding the optical fiber into the EP resin the characteristics during isothermal cure (gel point, vitrification) could be precisely detected due to changes in the fiber strain. In a follow up dynamic temperature scan the coefficient of thermal expansion and the glass transition temperature (T_g) of the fully cured EP were determined by the FBG sensor tech-

nique. All results obtained by the fiber optical method showed a very good agreement with those deduced by independent techniques, viz. rheological measurements, differential scanning calorimetry, and thermomechanical analysis. © 2007 Wiley Periodicals, Inc. *J Appl Polym Sci* 107: 719–725, 2008

Key words: strain; resins; curing of polymers; sensors; fibers

INTRODUCTION

Epoxy resins (EPs) are frequently used for several industrial applications such as matrices for composites, encapsulation or casting material in the electronic, and automotive or aircraft industries. For these purposes demanding properties are requested. The cure process of an EP resin is always combined with shrinkage due to chemical reactions. In consequence, cure-induced strains and thus stresses emerge in the cured material. This leads to a low performance, shape distortion, warpage, or even matrix cracking and delamination. The mechanical properties of EPs are strongly influenced by the thermal treatment during the cure process. Therefore, it is important to control and predict the chemical and physical processes for thermosetting resins during their cure schedule, including hardening and subsequent cooling of the material. The most interesting stage-dependant properties of the curing material are the actual conversion, the gel point, the glass transition temperature (T_g) as well as the cure-induced residual strains. During the cure process, the amount of chemical crosslinks, that is, the conversion of functional groups of resin and hardener, rises and a network is formed. At the gel point, the resin undergoes a phase transition from a liquid-like to a solid-like material. This is accompanied with the

formation of an infinite network. Several validated methods are known to determine the gel point, example, the time when the mechanical loss factor ($\tan \delta$) becomes independent of the frequency or the time when the storage shear (G') and loss moduli (G'') equal ($G' = G''$) in rheological measurements.^{1–5} After gelation, the crosslinking density is enhanced by further reactions. This is well reflected by the stiffness increase of the resin. At the end of the cure process, a partly or fully cured glassy thermoset is produced. The regions of liquid, solid, and glassy states are shown in detail in time-temperature-transition-diagrams of thermosets.^{4,6,7} If the temperature is kept constant and at a low level where unity conversion cannot be reached, the mobility of the molecules becomes hampered and the cure takes place diffusion-controlled. This leads to a vitrified, glassy, but not fully cured system. In case of isothermal cure, the vitrification is defined when the T_g and the cure temperature reach the same value. Note that T_g indicates the phase change of the resin from glassy to rubbery state and vice versa.

To control the material behavior of engineering parts their properties during the cure process as well as in the fully cured state should be investigated. This demands the use of different techniques. For the cure monitoring of resins usually differential scanning calorimetry (DSC), rheological measurements, dielectric analysis, and ultrasonic characterization methods are used.^{2,4,8–10} The shrinkage of the resin during a cure process can be well detected volumetrically by dilatometers.¹¹ The cure-induced strains (that later cause internal stresses) within the

Correspondence to: M. Harsch (margit.Harsch@de.bosch.com).

reacting material can be measured by optical fiber sensing techniques. Until now, this sensing principle is more frequently used to detect strains for structural integrity (detection of cracks, delaminations), process monitoring or quality control (effects of temperature cycles). This technique is also suited for the cure monitoring of thermosets being able to detect strains caused by mechanical forces (due to shrinkage) or thermal changes (because of expansion or contraction). There are already some works presenting the technique of fiber optical strain measurement in fiber-reinforced composite materials.^{12–17} Chehura et al.¹² used FBGs to detect strain development in different orientations in fiber-reinforced EP composites. O'Dwyer et al.¹³ compared the internal strain development in a carbon fiber composite under soft and harsh cure conditions by FBG-measurements and correlated the cure progress with results from dielectric measurements. The deposition of thin films on a substrate during cure was measured with fiber optical technique by Quintero et al.¹⁴ On the basis of the measured strains the authors were able to calculate the residual stresses in the film/substrate interface. Leng and Asundi¹⁵ compared the FBG sensor technique with extrinsic Fabry-Perot interferometry to follow the cure process in carbon/EP composites and found a good correlation between the related results. Interestingly, only few investigations address the cure process of pure EP resins. Merzlyakov et al.¹⁸ studied the cure- and thermally induced strains in a constrained EP resin in a steel tube by the use of an FBG sensor and estimated the emerging stresses within the material. Nicolais and co-workers investigated the cure of EP resins in several works^{19–21} by adopting fiber optical sensing. In one publication, the cited authors showed the changes in the refractive index as a function of degree of cure.¹⁹ The chemophysical transformations of an amine hardened EP resin were the topic of another work of this group²⁰ In a companion work, the nonisothermal cure procedure, cooling down, and demolding phases as well as internal strain relaxation in an EP resin were successfully investigated by this technique. Stress was applied to the resin because its cure took place in an aluminium mould to the walls of which the resin adhered. In a recent study,²¹ the stress and strain build-up during the nonisothermal cure of an EP resin were measured experimentally and calculated by considering a two-dimensional model.

In this work, we describe the use of the fiber optical sensing technique to monitor the cure-induced strains in EP resins during their cure cycle. The optical Fiber Bragg Grating (FBG) sensor was embedded in the curing resin. Recall that the mechanical (due to chemical reactions) as well as thermal deformations in the FBG surrounding material can be detected by this sensor. The aim of this study was to

determine characteristics (gel point, vitrification) of the EP resin during isothermal cure and in its cured stage [glass transition temperature, coefficient of thermal expansion (CTE)]. It should be emphasized that curing of the EP resin took place under free-shrinking condition so as to investigate the neat resin behavior without any influence of the surrounding recipient material. To assess the strain development in the curing resin without constraint effects, its free-shrinkage was ensured via lacking adhesion to the mould wall. The results received by the FBG sensor were compared and validated by those derived from independent techniques, viz. rheology, DSC, and thermomechanical analysis (TMA). Between the results of FBG sensing and traditional measurements a very good agreement was found.

THEORY OF FIBER BRAGG GRATINGS

FBG sensors are formed by modulating the refractive index of the core in an optical fiber. Inscription of Bragg gratings onto the fiber core can be realized by several methods such as interferometric, point-by-point, and phase-mask techniques.²² A schematic illustration of a Fiber Bragg Grating (FBG) sensor is shown in Figure 1.

A broadband spectrum light (Incident Spectrum) is guided along the core of the optical fiber. One particular wavelength λ_B is reflected at the gratings within the fiber core whereas the other part of the incident spectrum is transmitted through the fiber and reflected in a mirror at the fiber end. The wavelength reflected by the FBG, the Bragg wavelength λ_B , is dependent on the effective refractive index n_{eff} of the fiber, and the grating periodic spacing Λ , fulfilling the Bragg condition

$$\lambda_B = 2 \cdot n_{\text{eff}} \cdot \Lambda \quad (1)$$

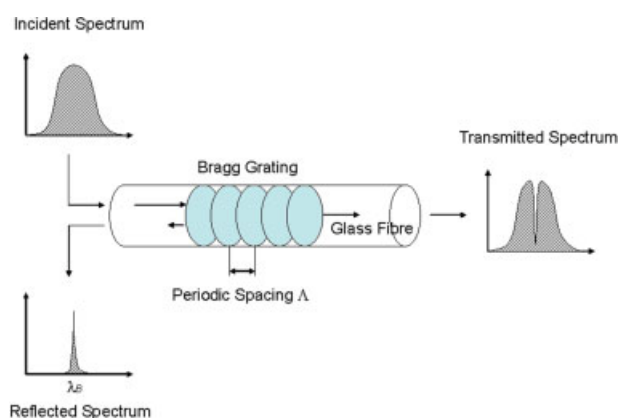


Figure 1 Principle of fiber bragg grating sensor (note that the reflection of the light is due to a mirror at the end of the glass fiber.) [Color figure can be viewed in the online issue, which is available at www.interscience.wiley.com.]

The effective index of refraction, as well as the periodic spacing between the grating planes, will be affected by changes in strain and temperature. Strain and temperature modulations, $\Delta\varepsilon$ and ΔT , respectively, lead to a shift in the reflected Bragg wavelength $\Delta\lambda_B$ which can be expressed with a relevant wavelength-strain-sensitive factor α and a wavelength-temperature-sensitive factor β which is given by

$$\Delta\lambda_B = \alpha \cdot \Delta\varepsilon + \beta \cdot \Delta T \quad (2)$$

Because of this measuring principle physical phenomena such as strain, temperature, and those connected with them (force, pressure) can be measured by the FBG sensor.²²

The Bragg gratings are inscribed in the glass fiber on a length of 5 mm. By embedding exactly this part of the fiber into a curing epoxy resin (EP) the stages of cure can be monitored. During the cure schedule the reacting resin contracts and applies pressure to the fiber optical sensor assuming an ideal coupling between EP and the glass fiber. This effect can be measured as shift in the reflected wavelength. The FBG sensing technique offers numerous advantages over the traditionally used methods. Because of its small diameter (ca. 125 μm) and chemical inertness the effective network building within the EP is hardly affected. Another beauty of this FBG method is that the outcome is independent on the geometry of the sample and on the thermal profile set for its curing. However, due to the ideal coupling between the curing EP and the fiber the two components are connected irreversibly and cannot be separated without mechanical destruction. Therefore the FBG sensor is not recoverable and suitable for single use only.

EXPERIMENTAL DETAILS

Material and cure parameters

In this study, a commercial Bisphenol A-based EP resin (Araldit MY 740) was cured with a mixture of two commercial anhydrides, methyl hexahydrophthalic anhydride, and hexahydrophthalic anhydride as hardener (all supplied by Huntsman, Basel, Switzerland). The mass ratio of resin to hardener was 100 : 83. Additionally, this resin composition contained of about 50 wt % inorganic filler on base of calcium silicate and calcium carbonate. Because of the presence of a high content of inorganic filler (that cause a better heat deduction) a bigger quantity (ca. 20 ml) of reacting material could be taken without exaggeration of temperature due to exothermic effects.

A homogenous mixture of resin, hardener, and filler was prepared by stirring, followed by degassing

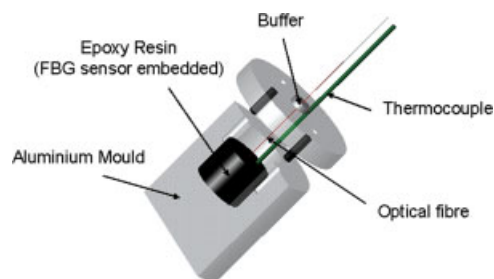


Figure 2 Measurement set-up with aluminium mould, EP sample, and FBG sensor. [Color figure can be viewed in the online issue, which is available at www.interscience.wiley.com.]

and preheating to 60°C. Afterwards, 20 ml EP resin was placed into a nonadhering cylindrical aluminium mould (preheated for cure temperature and equipped with an FBG sensor) and cured under isothermal conditions at temperatures of 70, 75, 80, and 90°C, respectively, for 1100 min. The cylindrical geometry of the heating tool was expected to provide a uniform heat distribution within the sample. After isothermal cure the glassy material was removed from the mould and afterwards postcured at 130°C for 120 min. This treatment resulted in a fully cured EP. In a subsequent dynamic run, the EP was heated from 40 to 190°C, kept at 190°C for 120 min, and afterwards cooled to ambient temperature. The heating and cooling rates were 0.5°C/min, respectively. The measurement device is shown schematically in Figure 2.

FBG sensor measuring system

The strain build evolution was measured by embedding a single FBG sensor within the EP resin along the vertical central line of the cylindrical aluminium mould cavity (cf. Fig. 2). The sensor was illuminated using the output from a light source with a central wavelength of 1549 nm. The reflected spectrum was detected by an optical spectrum analyzer and the information of the wavelength shift was transferred to an evaluating processor unit. Note that the Bragg wavelength shift also contains a contribution from the temperature. To consider the thermally induced shift in wavelength, a thermocouple was embedded in the EP resin next to the FBG sensor measuring the local temperature. The Bragg spectra along with the temperature were registered and saved every second. The resulted wavelength shift data were corrected by eliminating the temperature-caused signal change in the FBG (cf. eq. 2). The optical set-up can be seen in Figure 3.

Rheological measurements

The rheological measurements were performed on a Haake RS 1 (Thermo Electron, Karlsruhe) rheometer

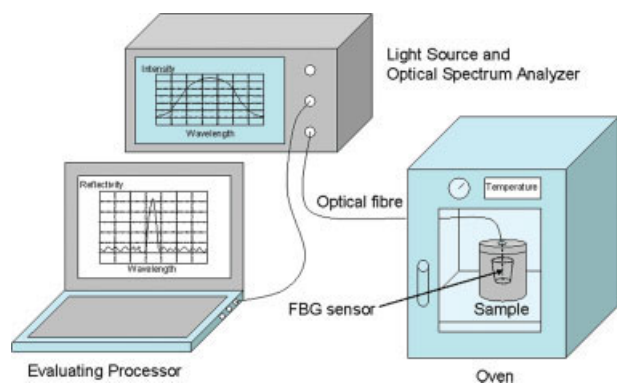


Figure 3 Optical set-up. [Color figure can be viewed in the online issue, which is available at www.interscience.wiley.com.]

equipped with a thermocontroller TCP/P using 60 mm diameter parallel plates with a gap of 0.5 mm. Experiments were carried out under oscillatory conditions applying an angular frequency of 10 rad/s and an amplitude of 5%. The EP composition to be cured was placed into the preheated device and cured isothermally at 70, 75, 80, and 90°C, respectively, until a glassy cured material was reached. The courses of the storage (G') and loss (G'') moduli were recorded as a function of the reaction time. The gel time was determined at the crossover of G' and G'' .

Differential scanning calorimetry

Conversion and glass transition temperature of specific specimens were investigated by means of differential scanning calorimetry (DSC) measurements. The experiments were carried out in a Mettler Toledo DSC 821^e (Giessen, Germany) module equipped with an intracooler. For reference purpose, a resin/hardener/filler sample was cured in a dynamic scan under nitrogen flow from -65 up to 300°C by applying a heating rate of 10°C/min. The integration of the corresponding exothermic peak resulted in a total heat of reaction of 175 J/g. This was considered to correspond to full (unity) conversion. All samples previously cured in an oven under isothermal conditions for different holding times using FBG were also subjected to the above mentioned dynamic DSC-scans. The residual enthalpy compared with the reference value indicated the missing conversion to reach unity. The T_g was determined at the inflection point of the baseline-step in the dynamic heat flow measurement.

Thermomechanical analysis

To detect the coefficient of thermal expansion (CTE) of the fully cured resin thermomechanical analysis

(TMA) experiment was carried out in a TMA/SS 6100 of Seiko Instruments (Neu Isenburg, Germany). A specimen cube of $3 \times 3 \times 3 \text{ mm}^3$ was placed between parallel plates of this device (surface of 10 mm² each) and loaded with 0.1 N. In the temperature range between -50 and 250°C, the sample was heated in a dynamic scan applying a rate of 2 °C/min.

RESULTS

During the isothermal cure of the EP resin, the cure-induced strain in the material was detected with the FBG sensor. It should be noted, that measuring device allowed a stress-free shrinkage of resin as it did not adhere to the moulding wall. So the detected strains (after deducting the thermally induced contribution) report on the cure-induced behavior of the EP composition without any influence of the surrounding aluminium mould. The strain development as a function of cure temperature and time are shown in Figure 4.

As expected, at the beginning of the isotherm there are no strains since cure shrinkage is relieved by liquid flow. After a certain time the strain curves tend to go downwards indicating a contraction in the optical fiber. The downward trend of the strain signal occurs linearly before it reaches some plateau. Comparing the runs, the strain build-up starts faster and the related change is steeper with increasing cure temperature. This is owing to the faster cure kinetics at elevated temperatures. A slight upward trend can be seen in the plateau-region for cure temperatures higher than 70°. This could be due to relaxation effects of the force of the EP that presses on the fiber caused by network building.

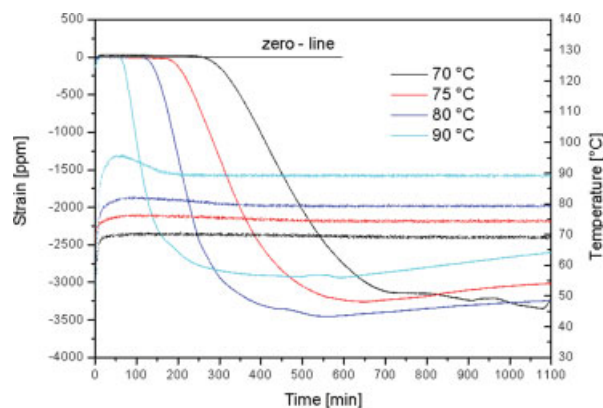


Figure 4 Strain development of the curing EP resin plotted against time under isothermal cure condition of 70, 75, 80, and 90°C, respectively. [Color figure can be viewed in the online issue, which is available at www.interscience.wiley.com.]

The polymeric network grows by intermolecular reactions that initially occur in the liquid state before a critical degree of three-dimensional structure (gel point) are reached. At this point, an infinite network is formed and the polymeric system begins to act as a solid capable to transfer static stresses. So, the time of the first strain change in the optical fiber can be used for determination of the gel point. It was assigned to a strain value differing more than 10 ppm from the base (zero) line. The gel times defined as described above were compared with those derived from rheological experiments. Recall that here the gel point was read as the crossover of the shear storage (G') and loss (G'') moduli. The results of both FBG and rheology methods are colated in Figure 5.

It is evident that time of the first strain appearance in fiber optical measurements is slightly shorter for all investigated temperatures, but generally in very good accordance with the gel time determined by rheological tests.

To get a deeper insight in the EP cure its isothermal cure at 75°C was followed as a function of time in DSC measurements and the evolution of conversion and T_g were detected. Consequently, it was possible to plot the actual degree of cure and strain in the same graph to find further correlations between them. By this way, characteristic points of the strain-time curve could be identified. The results are shown in Figure 6.

Conversion and T_g show similar and expected runs over the time. A linear raise in both curves is seen before they tend to reach a plateau with end values of 0.8 in conversion and 95°C in T_g . In the present study, the conversion at the first measurable strain signal (after 160 min) was found to be 0.35. This result is in line with cure kinetic studies of this EP system (not reported here) where a cure tempera-

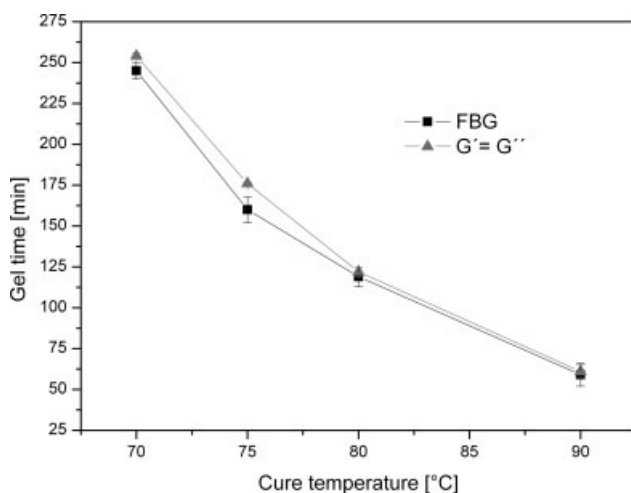


Figure 5 Gel time of the EP resin as function of cure temperature for FBG and rheology measurements, respectively.

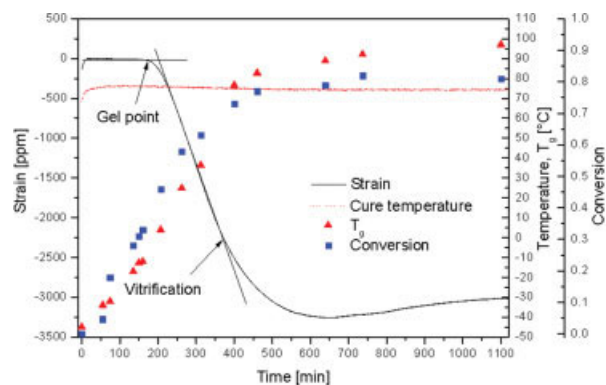


Figure 6 Strain, conversion and glass transition temperature development of the curing EP resin as function of time for isothermal cure at 75°C. [Color figure can be viewed in the online issue, which is available at www.interscience.wiley.com.]

ture-independent gel conversion of 0.38 was established. A deviation from the linear fall in the strain signal was noticed after 380 min. Note that at that time the T_g reaches the same value as the cure temperature, viz. 75°C. This indicates the vitrification of the material. In a vitrified system further crosslinking reactions may take place only by diffusion processes. So the slowing down of the crosslinking reactions and reaching an end-conversion less than unity can be explained. After vitrification also the strain signal should show a less steep change, which is the fact, indeed. So, based on Figure 6 changes in the strain signal of the FBG sensor can be assigned to characteristics of the cure (viz. gelation and vitrification) by considering the courses of the conversion and T_g of the curing EP assessed via DSC measurements.

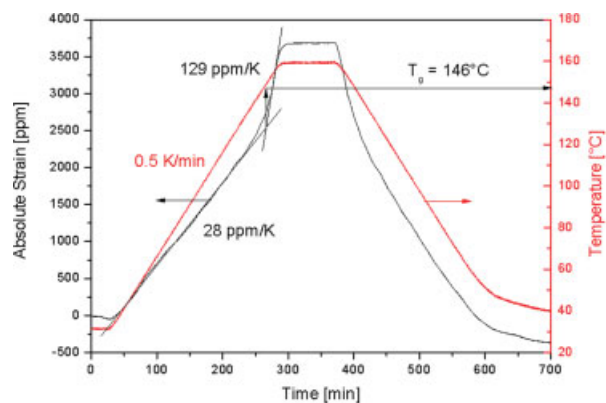


Figure 7 Strain plotted against time for the fully cured EP resin under dynamic temperature condition with a heating and cooling rate of 0.5 K/min measured by an FBG sensor. [Color figure can be viewed in the online issue, which is available at www.interscience.wiley.com.]

After the isothermal cure of the sample and its removal from the aluminium mould all investigated glassy samples (containing the embedded FBG sensor) were subsequently cured at 130°C to reach a fully cured stage. Afterwards, the samples were heated from 40 up to 190°C and then cooled by detecting simultaneously their thermal expansion behavior with the FBG sensor. For comparison purpose, samples of fully cured material were measured by thermomechanical analysis (TMA) in a temperature range from -50 to 250°C. The related results are presented in Figures 7 and 8, respectively.

Figure 7 displays the thermal expansion behavior of the cured EP resin measured via the strain signal of the FBG sensor and temperature via thermocouple and is plotted against time. In Figure 8, the thermal expansion from the TMA-measurements for the same EP resin is seen. The coefficient of thermal expansion (CTE) can be calculated by considering the related slopes of the curves. A change in the slope reflects the T_g , which is well resolved in the corresponding curves of both methods.

In Table I the T_g and CTE, below and above T_g , are listed for FBG, TMA, and DSC-measurements. Results show that the technique of fiber optical sensing yields very similar results as the well established methods of TMA and DSC with respect to CTE and T_g of the cured EP. So the confidence interval of the glass fiber measurement is given over a high temperature range from ambient temperature up to 190°C. This thermal treatment leads to an absolute strain of 3700 ppm in the investigated material which was suffered by the optical fiber without any debonding effects.

The FBG sensor seems to be an excellent tool not only to detect cure-induced strains in a reacting material but also for strain changes due to thermal effects.

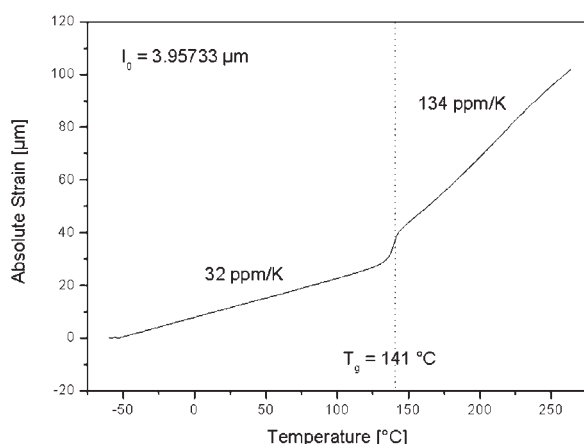


Figure 8 Strain plotted against temperature for the fully cured EP resin under dynamic temperature condition with a heating rate of 2 K/min measured by TMA.

TABLE I
 T_g and CTE for FBG, TMA, and DSC of the Fully Cured EP Resin

	T_g (°C)	CTE (ppm/K)	
		($T < T_g$)	($T > T_g$)
FBG	146	28	129
TMA	141	32	134
DSC	144	–	–

CONCLUSION

In this article, we were able to monitor the cure and temperature-induced strains during the cure cycle and in a subsequent temperature profile of the fully cured EP resin by using a Fiber Bragg Grating (FBG) sensing technique. Under isothermal cure conditions the characteristic points of the curing EP resin (gel point, vitrification) as well as these of the cured material (glass transition temperature, thermal expansion coefficient) via dynamic temperature scans could be precisely detected. The FBG results were in a very good agreement with those deduced by traditional methods, viz. rheological experiments, differential scanning calorimetry (DSC), and thermomechanical analysis (TMA). The fiber optical technique offers an excellent possibility to measure all characteristic points of a resin during and after cure by one single gauging without any dependency on geometry of the curing sample and temperature profile of the cure process provided that the thermally induced strains are considered accordingly.

References

1. Tung, C.-Y. M.; Dynes, P. J. *J Appl Polym Sci* 1982, 27, 569.
2. Mortimer, S.; Ryan, A. J.; Stanford, J. L. *Macromolecules* 2001, 34, 2973.
3. Pichaud, S.; Duteurtre, X.; Fit, A.; Stephan, F.; Maazouz, A.; Pascault, J. P. *Polym Int* 1999, 48, 1205.
4. Halley, P. J.; Mackay, M. E. *Polym Eng Sci* 1996, 36, 5, 593.
5. Núñez-Regueira, L.; Gracia-Fernandez, C. A.; Gómez-Barreiro, S. *Polymer* 2005, 46, 5979.
6. Karger-Kocsis, J. In *Handbuch Verbundwerkstoffe Werkstoffe*; Neitzel, M.; Mitschang, P., Eds.; Carl Hanser Verlag: München, Wien, 2004; pp 33.
7. Núñez, L.; Fraga, F.; Castro, A.; Núñez, M. R.; Villanueva, M. *Polymer* 2001, 42, 3581.
8. Prime, R. B. In *Thermosets*; Turi, E. A., Ed.; Academic Press: New York, 1981; p 453.
9. Barton, J. M. In *Advances in Polymer Sciences*; Dusek, K., Ed.; Springer: Berlin, 1985; p 111.
10. Holst, M.; Schänzlin, K.; Wenzel, M.; Xu, J.; Lellinger, D.; Alig, I. *J Polym Sci: Part B: Polym Phys* 2005, 43, 2314.
11. Snow, A. W.; Armistead, J. P. *J Appl Polym Sci* 1994, 52, 401.
12. Chehura, E.; Skordos, A. A.; Ye, C.-C.; James, S. W.; Partridge, I. K.; Tatam, R. P. *Smart Mat Struct* 2005, 14, 354.

13. O'Dwyer, M. J.; Maistros, G. M.; James, S. W.; Tatam, R. P.; Partridge, I. K. *Meas Sci Technol* 1998, 9, 1153.
14. Quintero, S. M. M.; Quirino, W. G.; Triques, A. L. C.; Valente, L. C. G.; Braga, A. M. B.; Achete, C. A.; Cremona, M. *Thin Solid Films* 2006, 494, 141.
15. Leng, J. S.; Asundi, A. *Smart Mat Struct* 2002, 11, 249.
16. Botsis, J.; Humbert, L.; Colpo, F.; Giaccari, P. *Opt Lasers Eng* 2005, 43, 491.
17. Murukeshan, V. M.; Chan, P. Y.; Ong, L. S.; Seah, L. K. *Sens Actuators* 2000, 79, 153.
18. Merzlyakov, M.; McKenna, G. B.; Simon, S. L. *Compos A* 2006, 37, 585.
19. Cusano, A.; Breglio, G.; Giordano, M.; Calabrò, A.; Cutolo, A.; Nicolais, L. *J Opt A: Pure Appl Opt* 2001, 3, 126.
20. Giordano, M.; Laudati, A.; Nasser, J.; Nicolais, L.; Cusano, A.; Cutolo, A. *Sens Actuators A* 2004, 113, 166.
21. Antonucci, V.; Cusano, A.; Giordano, M.; Nasser, J.; Nicolais, L. *Compos A* 2006, 37, 592.
22. Othonos, A.; Kalli, K. *Fiber Bragg Gratings*; Artech House: Boston, London, 1999; p 95.